NATIONAL ADVISORY COMMITTEE FOR AERONAUTICS

WARTIME REPORT

ORIGINALLY ISSUED

March 1942 as
Advance Restricted Report

WIND-TUNNEL INVESTIGATION OF EFFECT OF YAW ON LATERAL-STABILITY CHARACTERISTICS

IV - SYMMETRICALLY TAPERED WING WITH A CIRCULAR FUSELAGE HAVING A WEDGE-SHAPED REAR AND A VERTICAL TAIL

By I. G. Recant and Arthur R. Wallace

Langley Memorial Aeronautical Laboratory
Langley Field, Va.

NACA

WASHINGTON

NATIONAL ADVISORY COMMITTEE FOR AERONAUTICS

ADVANCE RESTRICTED REPORT

WIND-TUNNEL INVESTIGATION OF EFFECT OF YAW ON LATERAL-STABILITY CHARACTERISTICS

IV - SYMMETRICALLY TAPERED WING WITH A CIRCULAR FUSELAGE HAVING A WEDGE-SHAPED REAR AND A VERTICAL TAIL

By I. G. Recant and Arthur R. Wallace

SUMMARY

Combinations of an NACA 23012 tapered wing and a circular fuselage having a wedge-shaped rear were tested in the NACA 7- by 10-foot wind tunnel to determine the effect of wing-fuselage interference on the lateral-stability characteristics. The model configurations represented a high-wing, a midwing, and a low-wing monoplane. For each configuration, tests were made with a partial-span split flap neutral and deflected 60° and with and without a vertical tail. Tests of the fuselage alone and of the fuselage with the vertical tail were also made.

The results are presented in the form of increments of the rate of change in the coefficients of rolling moment, yawing moment, and lateral force with yaw caused by wing-fuselage interference. The coefficients at high angles of yaw for all model configurations are presented. The data are compared with similar model combinations of a tapered wing and circular fuselage with a pointed rear portion.

The interference effects on the combinations with the wedge-rear fuselage were similar to those on the combinations with the circular fuselage; that is, the interference reduced the effective dihedral of the low-wing model and increased the effective dihedral of the high-wing model, and the vertical tail was more effective on the low-wing combination than on the high-wing combination.

When the flap was neutral, the influence of interference on effective dihedral was greater for the circular-fuselage combinations than for the wedge-rear-fuselage combinations. When the flap was deflected, the effect of the interference on the dihedral was more favorable for the wedge-rear-fuselage combinations than for the circular-fuselage combinations. The directional stability of the model without tail with the wedge-rear fuselage was more favorably affected by wing-fuselage interference than the stability of those combinations with the circular fuselage, but the interference had a more favorable effect on the effectiveness of the vertical tail of the circular-fuselage models than on that of the wedge-rear-fuselage models.

At high angles of yaw the wedge-rear fuselage alone was more stable directionally than the circular fuselage alone.

INTRODUCTION

Data are available for evaluating the effect of the aerodynamic interference between wing and fuselage and between wing and vertical tail on the lateral-stability characteristics for certain types of model. The effects of interference on the characteristics of four types of wing having a partial-span split flap, both neutral and deflected, in combination with a circular fuselage are given in references 1 and 2. A comparison of a circular and an elliptical fuselage is shown in reference 2. The effect of the vertical position of the wing on the fuselage is given in references 1 and 2, and the effect of the longitudinal position of the wing on the fuselage is given in reference 3.

It was thought desirable to extend this investigation by tests of a fuselage of circular cross section but tapering to a knife edge (wedge rear) at the rear, because this shape is representative of a commonly used fuselage. Tests (reference 4) have shown that this type of fuselage is more stable, directionally, than a circular fuselage at large angles of yaw.

The present report gives the results of tests of a wedge-rear fuselage in combination with a wing at three vertical positions on the fuselage. Each combination was tested with and without a vertical tail and with and without a partial-span split flap deflected 60°.

MODEL AND APPARATUS

The tests were made in the NACA 7- by 10-foot wind tunnel with the regular six-component balance. The tunnel and the balance are described in references 5 and 6.

The model (fig. 1) was identical with the circular fuselage and symmetrically tapered wing model of reference 2 except for the new shape of the fuselage rear. For the midwing combination the chord line of the wing was placed on the center line of the fuselage. For the high- and the low-wing combinations the outer surface of the wing was made tangent to the respective surfaces of the fuselage. The wing was set at 0° incidence with respect to the fuselage center line for all cases.

The 3:1 symmetrically tapered wing used in the tests was previously used in the investigation reported in reference 7. It has the NACA 23012 section and the maximum upper-surface ordinates are in one plane, giving the chord plane a dihedral of 1.45°. The wing tips are formed of quadrants of approximately similar ellipses. The sweepback of the locus of one-quarter-chord points is 4.75°, the area is 4.1 square feet, and the aspect ratio is 6.1.

The fuselage is the same as the circular fuselage used in the investigations reported in references 1, 2, 3, and 8 except that the thickness in side elevation is increased back of the 28-inch station in such a way that the fuselage terminates in a vertical line instead of in a point. The ordinates of the fuselage, which will hereinafter be referred to as the wedge-rear fuselage, are given in table I.

A new vertical tail was constructed for the new fuselage. It is of NACA 0009 section and has an effective area of 53.7 square inches measured to the center line of the fuselage. (See fig. 1.) The aspect ratio of the vertical tail is 2.2, based on the area as defined and on the tail span to the center line of the fuselage. The tail area and the aspect ratio are the same as for the vertical tail used on the circular fuselage discussed in previous papers of this stability-investigation series.

Split flaps, 20 percent of the wing chord and 60 percent of the wing span, were made of 1/16-inch steel. For the high-wing and the midwing combinations, the flaps were cut to allow for the fuselage, and the gaps between the fuselage and the flaps were sealed. The flaps were attached with suitable angle blocks at a deflection of 60°.

TESTS

The test procedure was similar to that used in previous investigations (references 2 and 3). Tests were made of the model with and without the flaps and with and without the vertical tail for all wing positions. All combinations were tested at angles of attack from -10° to 20° with the model yawed -5°, 0°, and 5°. A yaw range of -15° to 50° was investigated for each combination at an angle of attack 2° less than the angle of attack for maximum lift at 0° yaw.

A dynamic pressure of 16.37 pounds per square foot, which corresponds to a velocity of 80 miles per hour under standard conditions, was maintained in all tests. The Reynolds number based on a mean wing chord of 9.84 inches was about 609,000. Based on a turbulence factor of 1.6 for the 7- by 10-foot wind tunnel, the effective Reynolds number was about 975,000.

RESULTS

The data are given, in standard nondimensional coefficient form, with respect to the stability axes and the center-of-gravity location shown in figure 1. The stability axes are a system of axes in which the X axis is the intersection of the plane of symmetry of the airplane with a plane perpendicular to the plane of symmetry and parallel to the relative wind direction, the Y axis is perpendicular to the plane of symmetry, and the Z axis is in the plane of symmetry and perpendicular to the X axis. The results of all former reports in this series were given with respect to the wind axes. Data taken from these reports and presented herein have, therefore, been converted to the stability axes. The stability axes are used because, with the stability axes, rolling-moment data are automatically corrected for untrimmed pitching moments and are less likely to lead to false conclusions.

The coefficients for the fuselage alone and for the fuselage with vertical tail are based on the wing dimensions. The coefficients are defined as follows:

C_L lift coefficient (L/qS)

C_D drag coefficient (D/qS)

C_m pitching-moment coefficient $(M/q\bar{c}S)$

C_Y lateral-force coefficient (Y/qS)

C_{Y_ψ} slope of curve of lateral-force coefficient against yaw $(\partial C_Y/\partial\psi)$

C_l rolling-moment coefficient (L/qbS)

C_{l_ψ} slope of curve of rolling-moment coefficient against yaw $(\partial C_l/\partial\psi)$

C_n yawing-moment coefficient (N/qbS)

C_{n_ψ} slope of curve of yawing-moment coefficient against yaw $(\partial C_n/\partial\psi)$

Δ_1 change in partial derivatives caused by wing-fuselage interference

Δ_2 change in vertical tail effectiveness caused by wing-fuselage interference

where

L lift, rolling moment

D drag

Y lateral force

M pitching moment

N yawing moment

q dynamic pressure $(\frac{1}{2}\rho V^2)$

V tunnel air velocity

ρ air density

S wing area

b wing span

$\bar{c}$ average wing chord

and

α angle of attack corrected to free stream, degrees

α' wind-tunnel angle of attack, degrees

ψ angle of yaw, degrees

δ_f angle of flap deflection, degrees

Λ angle of wing sweep, degrees

Lift, drag, and pitching-moment coefficients for the various wing-fuselage arrangements are presented in figure 2. The values of α and C_D shown in this figure were corrected to free air, but in all subsequent figures no corrections to α' were made. The lateral-stability derivatives of component parts of the model appear in figure 3.

The increments of partial derivatives with respect to the angle of yaw of rolling-moment, yawing-moment, and lateral-force coefficients due to wing-fuselage interference Δ_1 and due to wing-fuselage interference on the vertical tail Δ_2 are shown in figures 4 to 9. The increment Δ_1 is the difference between the slope for the wing-fuselage combination without the tail and the sum of the slopes for the wing and the fuselage, each tested separately. Thus, Δ_1 is the change in C_{l_ψ}, C_{n_ψ}, and C_{Y_ψ} caused by wing-fuselage interference for the model without the tail. The increment Δ_2 is the difference between the slope produced by the vertical tail with the wing present and the slope produced by the vertical tail with the wing absent. The increment Δ_2 is, therefore, the change in effectiveness of the vertical tail caused by the addition of the wing to the fuselage. If, for example, the value of C_{n_ψ} for the complete model is desired, the following equation may be used:

$$C_{n_\psi} = C_{n_\psi}(\text{wing}) + C_{n_\psi}(\text{fuselage and tail}) + \Delta_1 C_{n_\psi} + \Delta_2 C_{n_\psi}$$

Values of C_{l_ψ} and C_{Y_ψ} for the complete model may be obtained in a similar manner.

The values of C_{l_ψ}, C_{n_ψ}, and C_{Y_ψ} used to compute Δ_1 and Δ_2 were obtained from tests at -5° and 5° yaw by assuming a straight-line variation between those points. This assumption has been shown in reference 1 to be valid except at high angles of attack. Tailed symbols on the curves of figures 3 to 9 were obtained from slopes measured from curves in figures 10 to 13.

The lateral-stability characteristics of the component parts of the model at high angles of yaw are given in figure 10 and the characteristics for the various combinations with and without the vertical tail at high angles of yaw are shown in figures 11 to 13.

DISCUSSION

General Comments

The lift, the drag, and the pitching-moment coefficients of the several model combinations are shown in figure 2. As is to be expected, the high-wing combinations are more stable in pitch than the low-wing combinations. Inasmuch as the tests were made without wing fillets, the data for the low-wing combinations show the effect of the burble at the wing-fuselage juncture. (See reference 3.)

Lateral Stability at Small Angles of Yaw

Component parts.- The wing-alone data given on figure 3 were taken from reference 7 and converted to the stability axes. The data of figure 3 show that the wing alone with flaps deflected is less stable in roll than with flaps neutral. The data of reference 7 show a reverse relationship. The difference is caused by the fact that the results of reference 7 were not corrected for the component of pitching moment, which was negligible for flaps neutral but appreciable for flaps deflected. Lateral force of the wing alone with respect to the stability axis is found to be small with flaps either neutral or deflected. When the moments of the wing alone are computed about points above and below the wing to represent the center-of-gravity position for high- and low-wing monoplanes, it was found, as is shown in figure 3, that the change in lateral-stability characteristics is very small.

The fuselage data are also given in figure 3 and are converted from data of reference 1 to the stability axes and corrected for the wing area used in this paper. Both fuselages give substantially similar results. The circular fuselage, however, is seen to be slightly less unstable in yaw than the wedge-rear fuselage. This result is in agreement with the data of reference 4 for small angles of yaw. The vertical tail is more effective in producing yawing moment in combination with the wedge-rear fuselage.

Wing-fuselage interference.- In general, the interference with the wedge-rear fuselage was very similar to the interference with the circular fuselage. There are, however, certain small differences, which it might be well to point out.

The increment $\Delta_1 C_{l_\psi}$ (fig. 4) for flap neutral is greater for the circular fuselage over most of the angle-of-attack range. For flaps deflected the opposite is true for the high wing and, over a small angle-of-attack range, for the low wing. Figure 4 shows the tendency for the flaps to increase $\Delta_1 C_{l_\psi}$ more when added to the wedge-rear-fuselage combination than when added to the circular-fuselage combination. The effect of the burble a few degrees before complete stall is clearly shown by the abrupt change in the curve for $\Delta_1 C_{l_\psi}$ for flap neutral. For flaps deflected, the burble occurs too close to the complete stall to show clearly in the curves, but it is probably responsible for the fact that the stall occurs 2° earlier for the low wing.

With flaps neutral the increment $\Delta_1 C_{l_\psi}$ (fig. 5) is more stabilizing for the wedge-rear fuselage for all three wing positions except for the midwing combination at angles of attack above 10° where the increment is about the same. The result is the same for the condition with the flap deflected except that, at angles of attack above 10°, the interference for the circular fuselage becomes more stabilizing.

The increment $\Delta_1 C_{Y_\psi}$ (fig. 6) is about the same for either fuselage, although it shows greater variation with angle of attack for the wedge-rear fuselage.

Effect of wing-fuselage interference on vertical tail.- The increment $\Delta_2 C_{l_\psi}$ (fig. 7) is rather small and erratic, as might be expected. The difference between the increments for the two fuselage shapes is much greater with the flap neutral than with the flap deflected.

The increment $\Delta_2 C_{n_\psi}$ (fig. 8) is, in general, more stabilizing for the circular fuselage than for the wedge-rear fuselage. The difference between the values of $\Delta_2 C_{n_\psi}$ for the two fuselages is most marked when the wing is in the low position. Flap deflection also increases the difference.

The lateral force increment $\Delta_2 C_{Y_\psi}$ is about the same for both fuselages for the low-wing arrangement. With the midwing combination, the wedge-rear fuselage has a more positive $\Delta_2 C_{Y_\psi}$, and with the wing in the high position, a much more positive (less negative) $\Delta_2 C_{Y_\psi}$.

Lateral Stability at Large Angles of Yaw

Component parts.- Rolling-moment coefficients (fig. 10(a)) due to the fuselage and to the fuselage with tail are small, as would be expected. Yawing moments (fig. 10(b)) of the fuselages alone at low angles of yaw are nearly the same. At high angles of yaw, the circular fuselage is more unstable. With the tail on, the range tested for the circular fuselage is too small to determine the difference at high angles of yaw but at low values of yaw the two fuselages are about the same. Lateral force (fig. 10(c)) for the fuselage alone is higher for the wedge-rear fuselage at high values of ψ. This condition is in agreement with the more stable yawing moments of the wedge-rear fuselage in this range. As the angle of attack is increased, the wedge-rear fuselage develops less lateral force and becomes more unstable at large angles of yaw.

The complete model.- The plots of rolling-moment coefficients (figs. 11(a), (b), (c), (d)) show again the favorable interference for the high-wing combination and unfavorable interference for the low-wing combination except for the low-wing combination with the flaps neutral. As may be seen in figure 4, this combination was tested at a greater angle of attack than the angle of attack at which the burble at the wing-fuselage juncture occurs. Because of the burble, the interference is as favorable for the low-wing combination as for the high-wing combination at small englee of yaw. The decrease in effective dihedral of the low-wing combination at large angles of yaw may be due to the tendency of the air flow to revert to the flow condition before the burble. This decrease is not caused by the stalling of one wing tip, because the lift decreased more rapidly with yaw for the high-wing combination, which did not exhibit the marked reduction in slope of the rolling-moment-coefficient curve shown by the low-wing combination. With flaps deflected, the low-wing combination has negative effective dihedral, as would be expected from the interference plots.

A comparison of the yawing-moment coefficients produced by the wedge-rear-fuselage model and the circular-fuselage model is made in figure 12. The circular-fuselage model had a wing with an angle of sweep of 14°. Data for this combination are given because it was the only circular-fuselage combination tested at an angle of yaw above 15°. Unpublished data have shown that the effect of sweep on yawing moment is small and should therefore not materially influence the comparison.

With the flaps neutral (fig. 12(a)), the wedge-rear fuselage is more stable up to about 22° yaw, although the difference in sweep of the wings tends to favor the circular-fuselage combination slightly. Beyond an angle of yaw of 22° there is not much difference between the two fuselage combinations. The stability of the wedge-rear combinations at large angles of yaw is not so great as would be expected from a comparison of the test results of the two fuselages alone. When the flaps are deflected (fig. 12(b)), the wedge-rear fuselage with the high-wing

L-520

combination shows greater stability than the circular fuselage, but with the low-wing combination both fuselages have about the same stability. The effect of flap deflection is probably greater than the effect of fuselage shape.

The lateral-force-coefficient curves (fig. 13) are quite regular. For flaps neutral there is no consistent difference between the two fuselage combinations. The deflection of flaps increases the lateral-force coefficient developed by the low-wing combination but does not materially change the characteristics of the high-wing combination.

CONCLUSIONS

For small angles of yaw there was very little difference between the lateral-stability characteristics of the wedge-rear fuselage and those of the circular fuselage. Some of the small differences were as follows:

1. The increments of rolling-moment coefficient due to wing-fuselage interference for flaps neutral were greater for the circuler fuselage, that is, were more stabilizing for the high-wing combination and more destabilizing for the low-wing combination.

2. With flaps deflected the increment of rolling moment due to wing-fuselage interference was more stabilizing for the wedge-rear fuselage for all model configurations.

3. The increment of yawing-moment coefficient due to wing-fuselage interference was more stabilizing for the wedge-rear-fuselage combination.

4. The effect of wing-fuselage interference on the vertical tail tended to make the circular-fuselage combination more stable directionally than the wedge-rear-fuselage combination regardless of wing position or flap deflection.

At large angles of yaw, the wedge-rear fuselage alone was more stable directionally than the circular fuselage but, in combination with the wing and the vertical tail, there was very little difference between the yawing-moment coefficients of the two fuselage combinations.

Langley Memorial Aeronautical Laboratory,
National Advisory Committee for Aeronautics,
Langley Field, Va.

REFERENCES

1. Bamber, M. J., and House, R. O.: Wind-Tunnel Investigation of Effect of Yaw on Lateral-Stability Characteristics. II - Rectangular N.A.C.A. 23012 Wing with a Circular Fuselage and a Fin. T.N. No. 730, NACA, 1939.

2. House, Rufus O., and Wallace, Arthur R.: Wind-Tunnel Investigation of Effect of Interference on Lateral-Stability Characteristics of Four NACA 23012 Wings, an Elliptical and a Circular Fuselage, and Vertical Fins. Rep. No. 705, NACA, 1941.

3. Recant, Isidore G., and Wallace, Arthur R.: Wind-Tunnel Investigation of Effect of Yaw on Lateral-Stability Characteristics. III - Symmetrically Tapered Wing at Various Positions on Circular Fuselage with and without a Vertical Tail. T.N. No. 825, NACA, 1941.

4. Hoggard, H. Page, Jr.: Wind-Tunnel Investigation of Fuselage Stability in Yaw with Various Arrangements of Fins. T.N. No. 785, NACA, 1940.

5. Harris, Thomas A.: The 7 by 10 Foot Wind Tunnel of the National Advisory Committee for Aeronautics. Rep. No. 412, NACA, 1931.

6. Wenzinger, Carl J., and Harris, Thomas A.: Wind-Tunnel Investigation of an N.A.C.A. 23012 Airfoil with Various Arrangements of Slotted Flaps. Rep. No. 664, NACA, 1939.

7. Bamber, M. J., and House, R. O.: Wind-Tunnel Investigation of Effect of Yaw on Lateral-Stability Characteristics. I - Four N.A.C.A. 23012 Wings of Various Plan Forms with and without Dihedral. T.N. No. 703, NACA, 1939.

8. Recant, Isidore G., and Wallace, Arthur R.: Wind-Tunnel Investigation of the Effect of Vertical Position of the Wing on the Side Flow in the Region of the Vertical Tail. T.N. No. 804, NACA, 1941.

TABLE I.- DIMENSIONS OF WEDGE-REAR FUSELAGE

Station (in.)	Radius (in.)	Depth (in.)
0	0	0
.312	.772	1.544
.812	1.242	2.484
1.312	1.572	3.144
2.312	2.044	4.088
4.312	2.650	5.300
8.312	3.238	6.476
12.312	3.410	6.820
16.312	3.440	6.880
20.312	3.406	6.812
24.312	3.268	6.536
28.312	2.990	5.980
32.312	2.516	5.134
34.312	2.170	4.710
36.312	1.698	4.287
38.312	1.000	3.863
39.312	.548	3.652
40.312	0	3.440

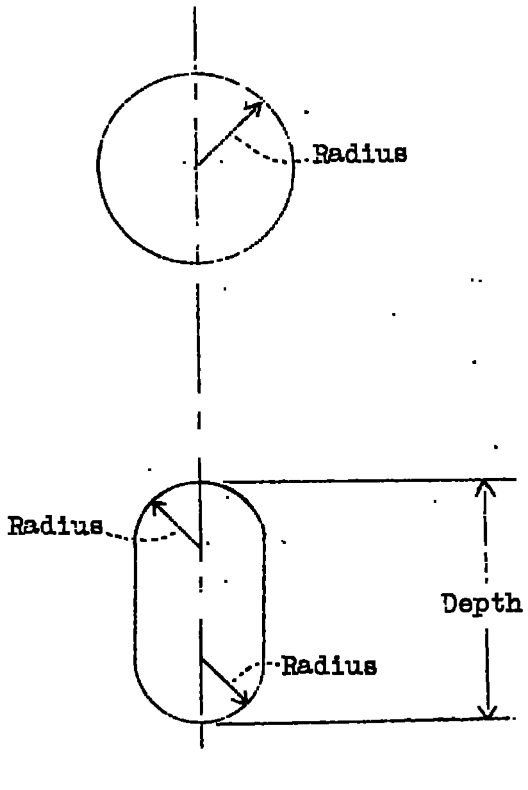

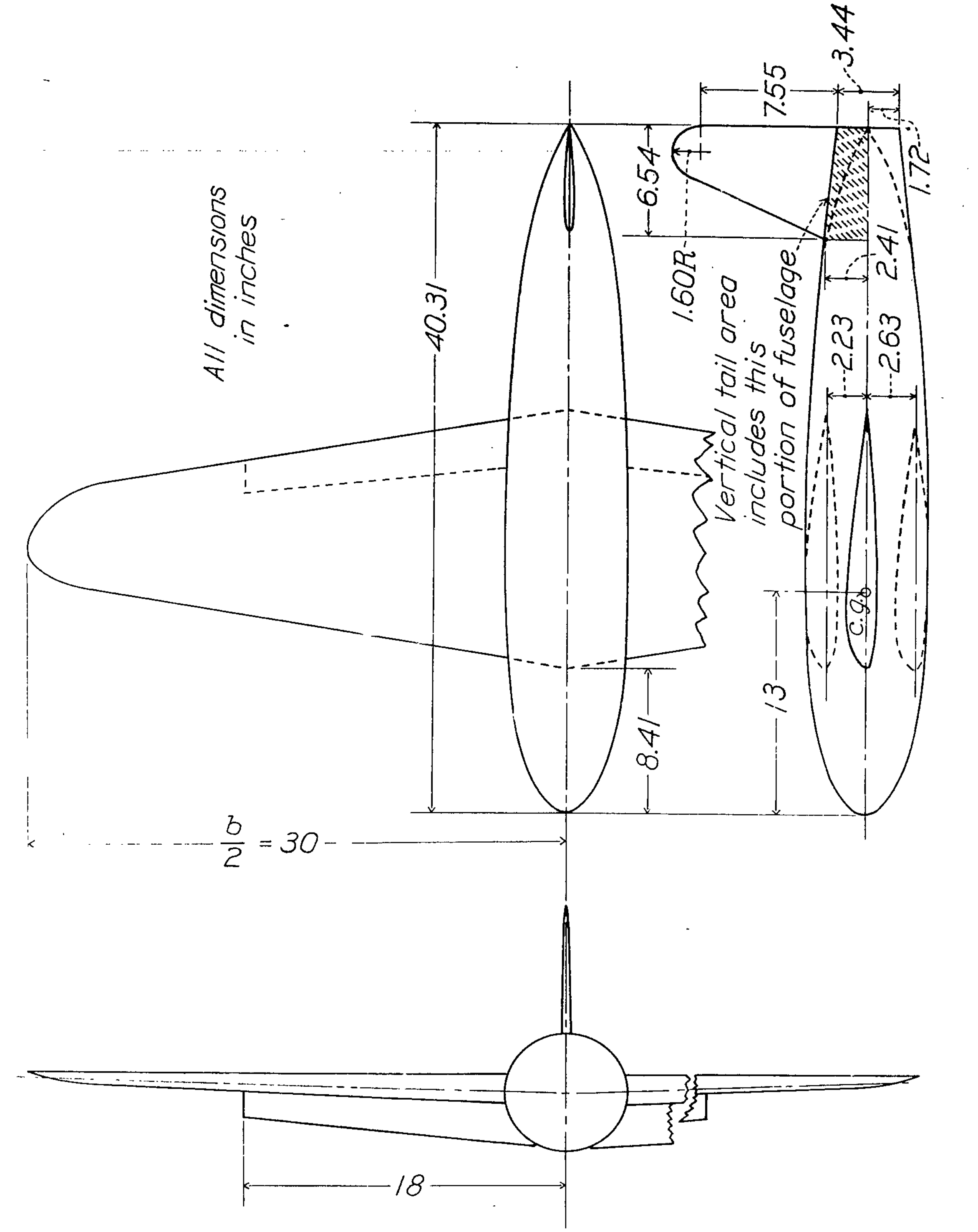

Figure 1.- NACA 23012 wing in combination with a wedge-rear fuselage and a tail of NACA 0009 section.

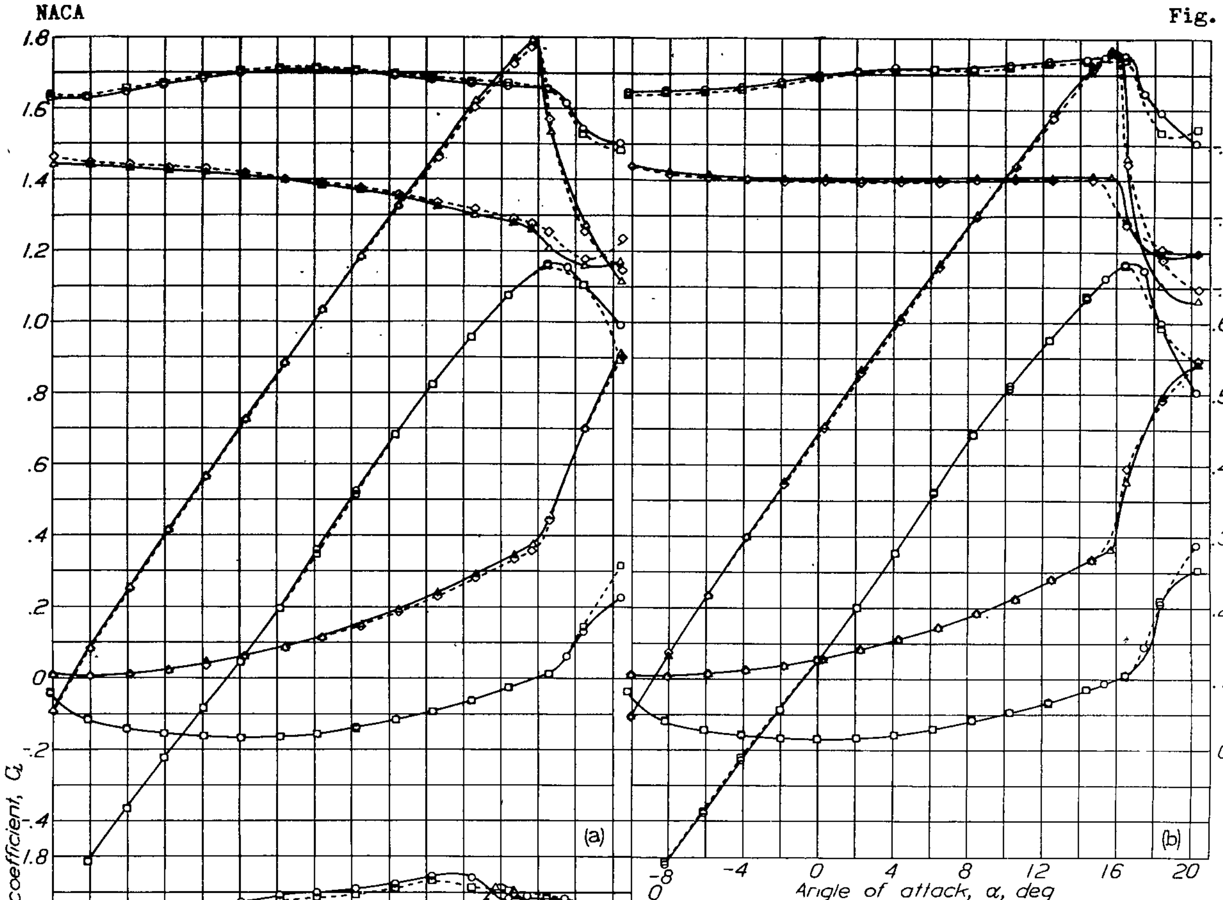

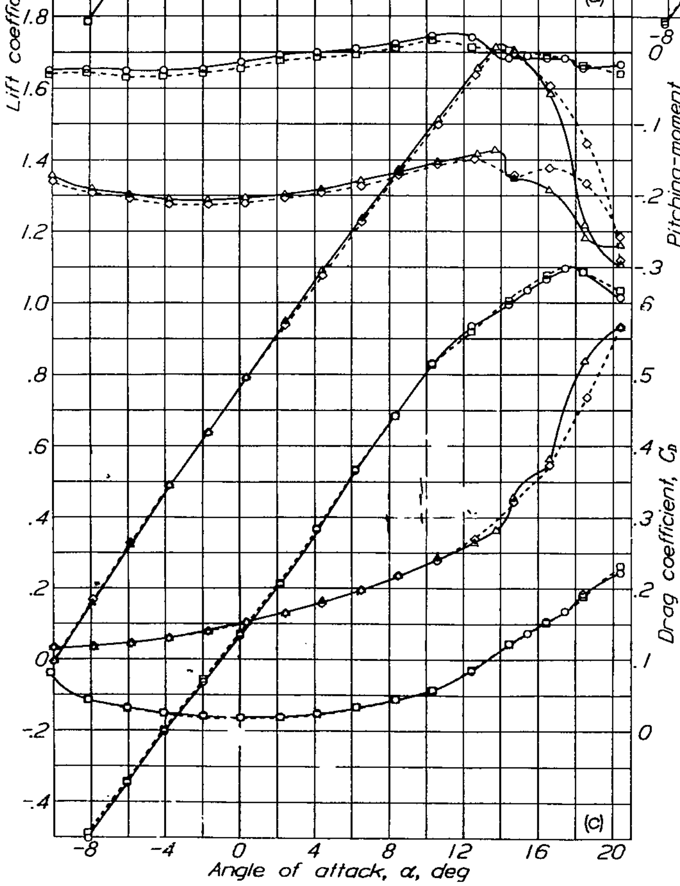

Symbol	○	□	△	◇
δ_f, deg	0	0	60	60
ψ, deg	0	5	0	5

(a) High wing position.
(b) Middle wing position.
(c) Low wing position.

Figure 2.- Lift, drag and pitching-moment coefficients of complete model. NACA 23012 wing with wedge-rear fuselage and vertical tail.

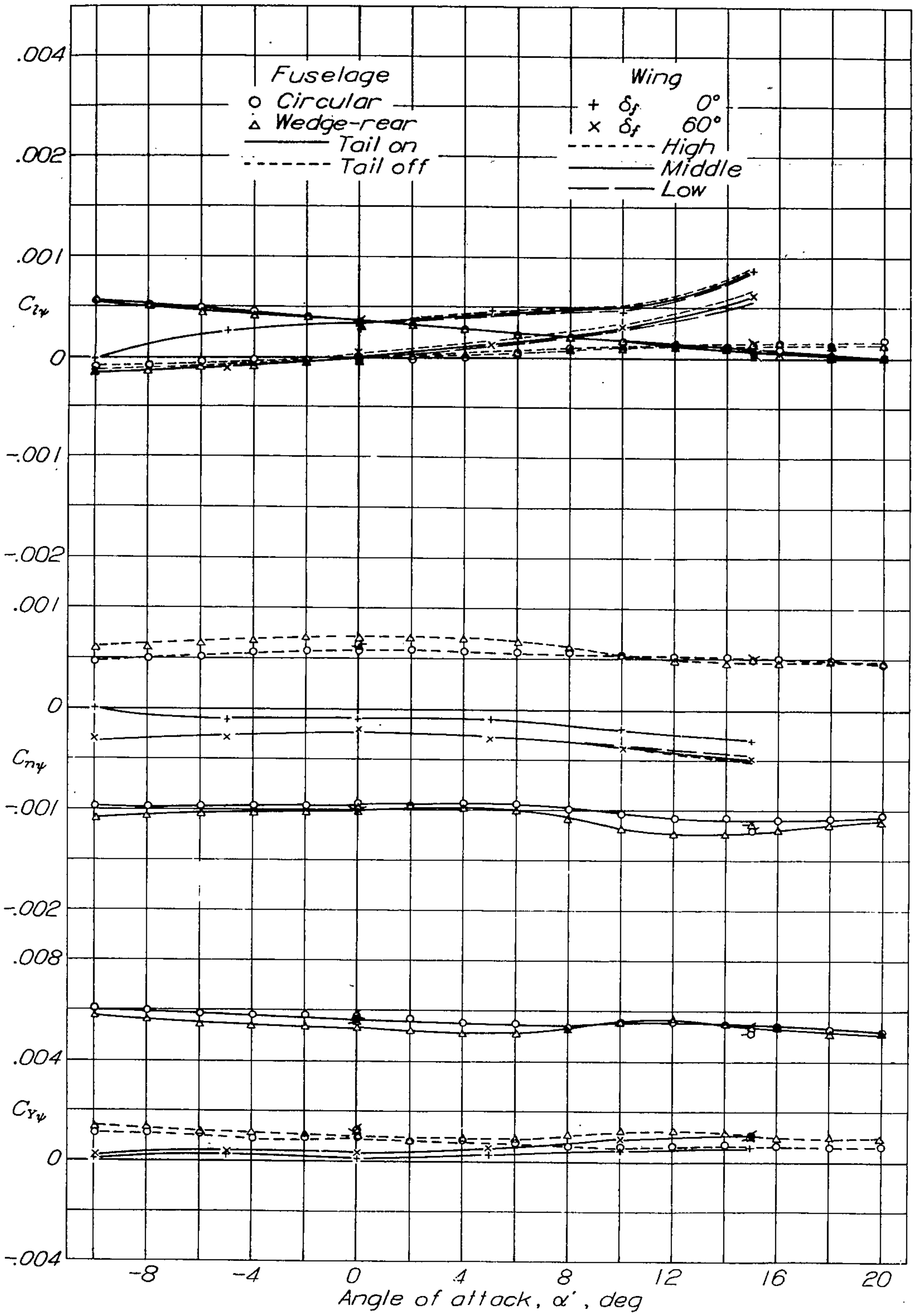

Figure 3.- Variation of C_{l_ψ}, C_{n_ψ}, and C_{Y_ψ} with angle of attack. NACA 23012 wing alone, fuselage alone, and fuselage with tail. (Data for wing and circular fuselage converted from references 7 and 1, respectively.)

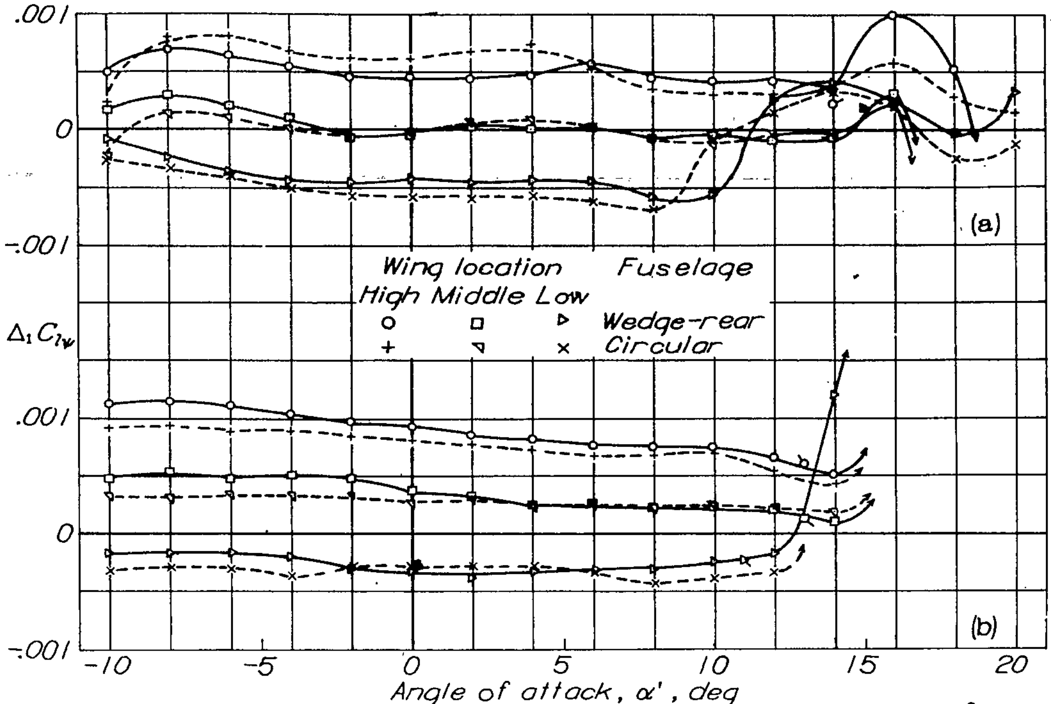

(a) δ_f, 0° (b) δ_f, 60°

Figure 4.- Increment of C_{l_ψ} due to wing-fuselage interference. NACA 23012 wing with fuselage. (Data for circular fuselage converted from reference 2.)

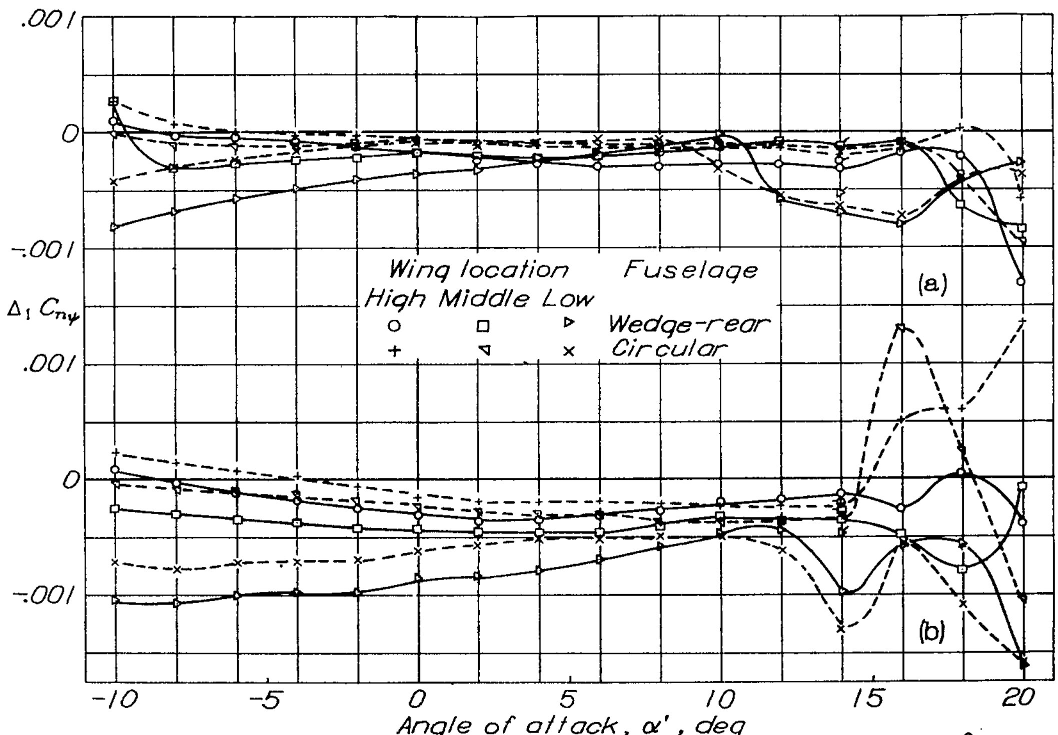

(a) δ_f, 0° (b) δ_f, 60°

Figure 5.- Increment of C_{n_ψ} due to wing-fuselage interference. NACA 23012 wing with fuselage. (Data for circular fuselage converted from reference 2.)

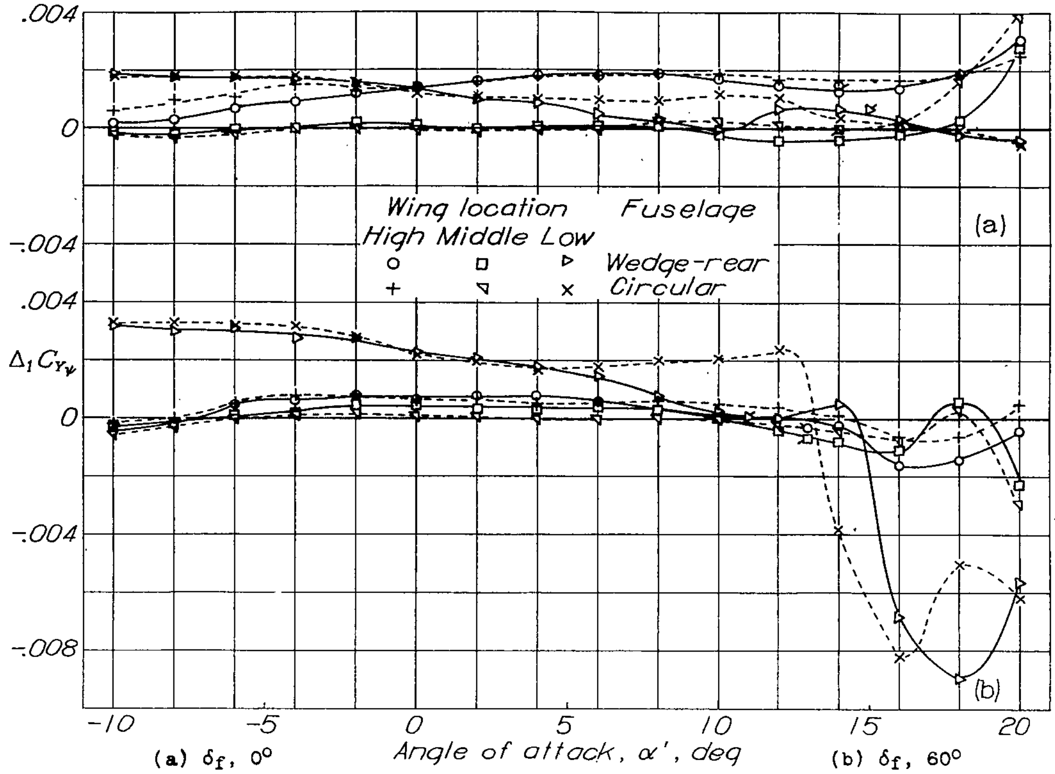

Figure 6.- Increment of C_{Y_ψ} due to wing-fuselage interference. NACA 23012 wing with fuselage. (Data for circular fuselage converted from reference 2.)

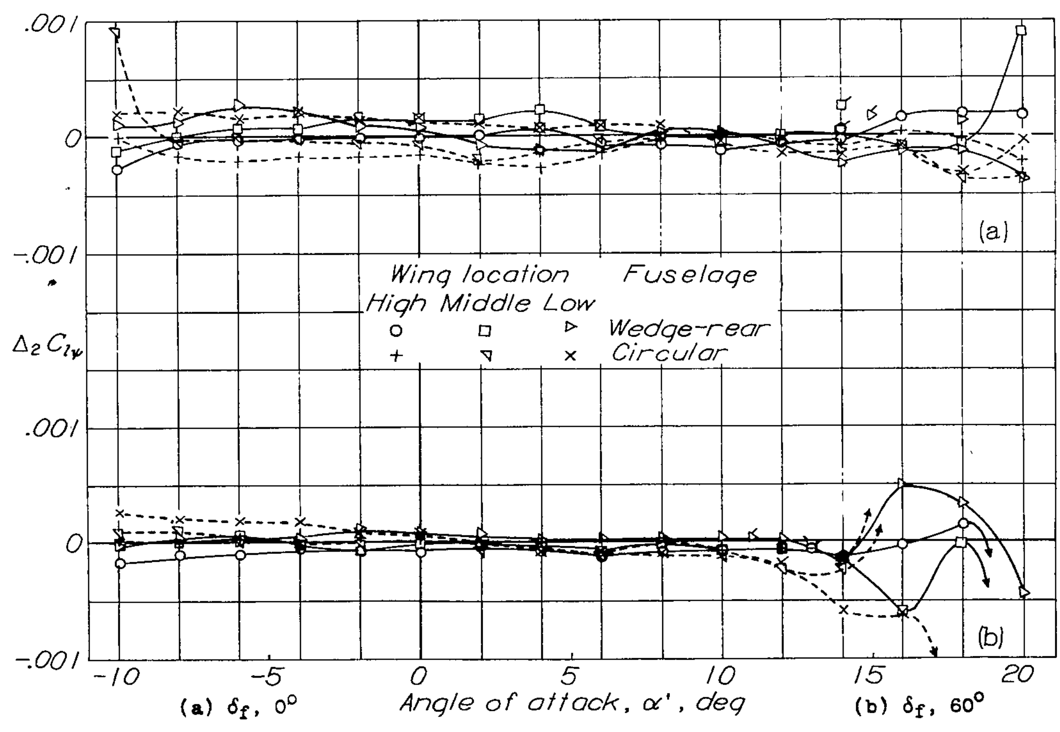

Figure 7.- Effect of wing-fuselage interference on C_{l_ψ} due to tail. NACA 23012 wing with fuselage and tail. (Data for circular fuselage converted from reference 2.)

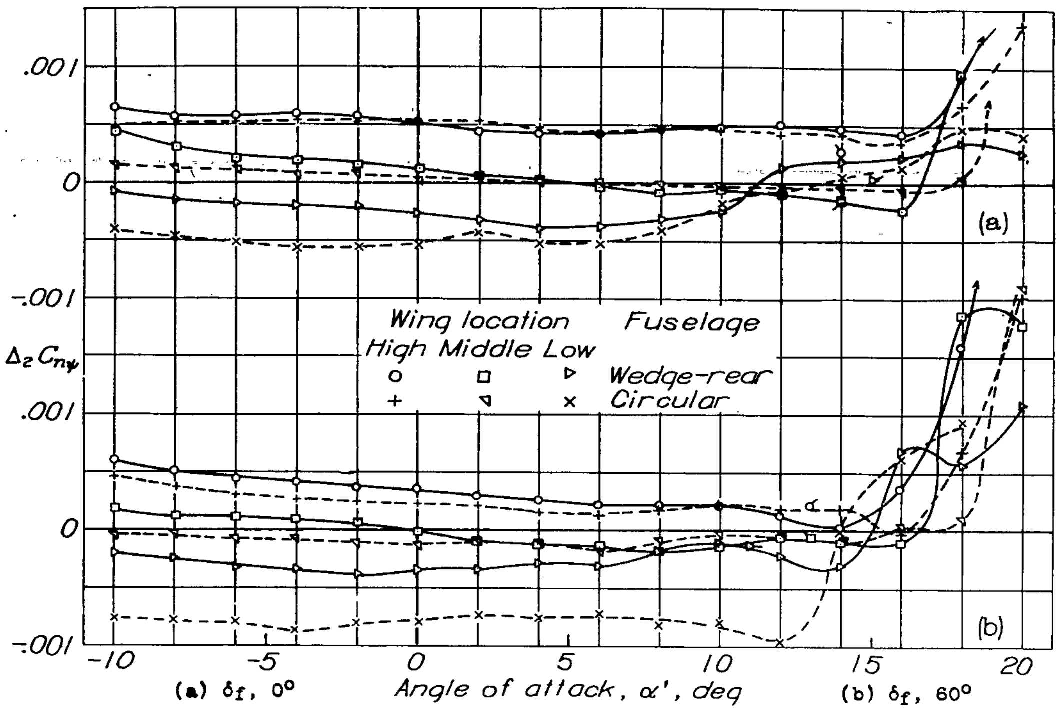

Figure 8.- Effect of wing-fuselage interference on C_{n_ψ} due to tail. NACA 23012 wing with fuselage and tail. (Data for circular fuselage converted from reference 2.)

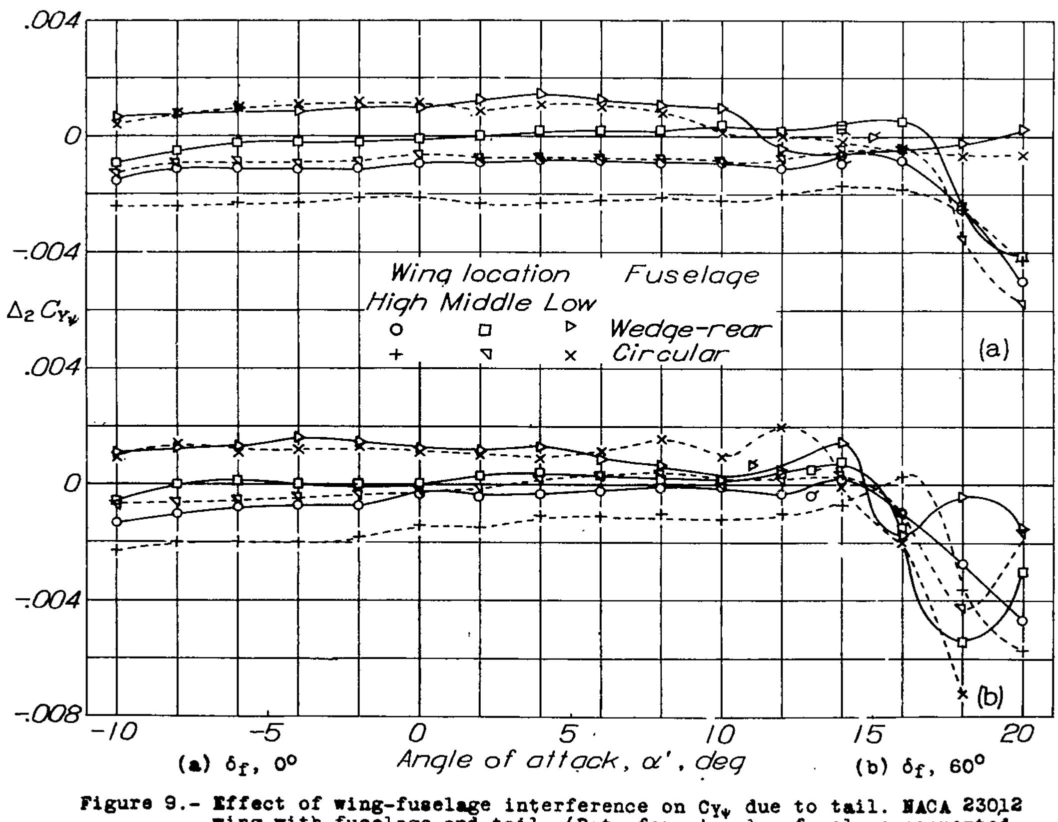

Figure 9.- Effect of wing-fuselage interference on C_{Y_ψ} due to tail. NACA 23012 wing with fuselage and tail. (Data for circular fuselage converted from reference 2.)

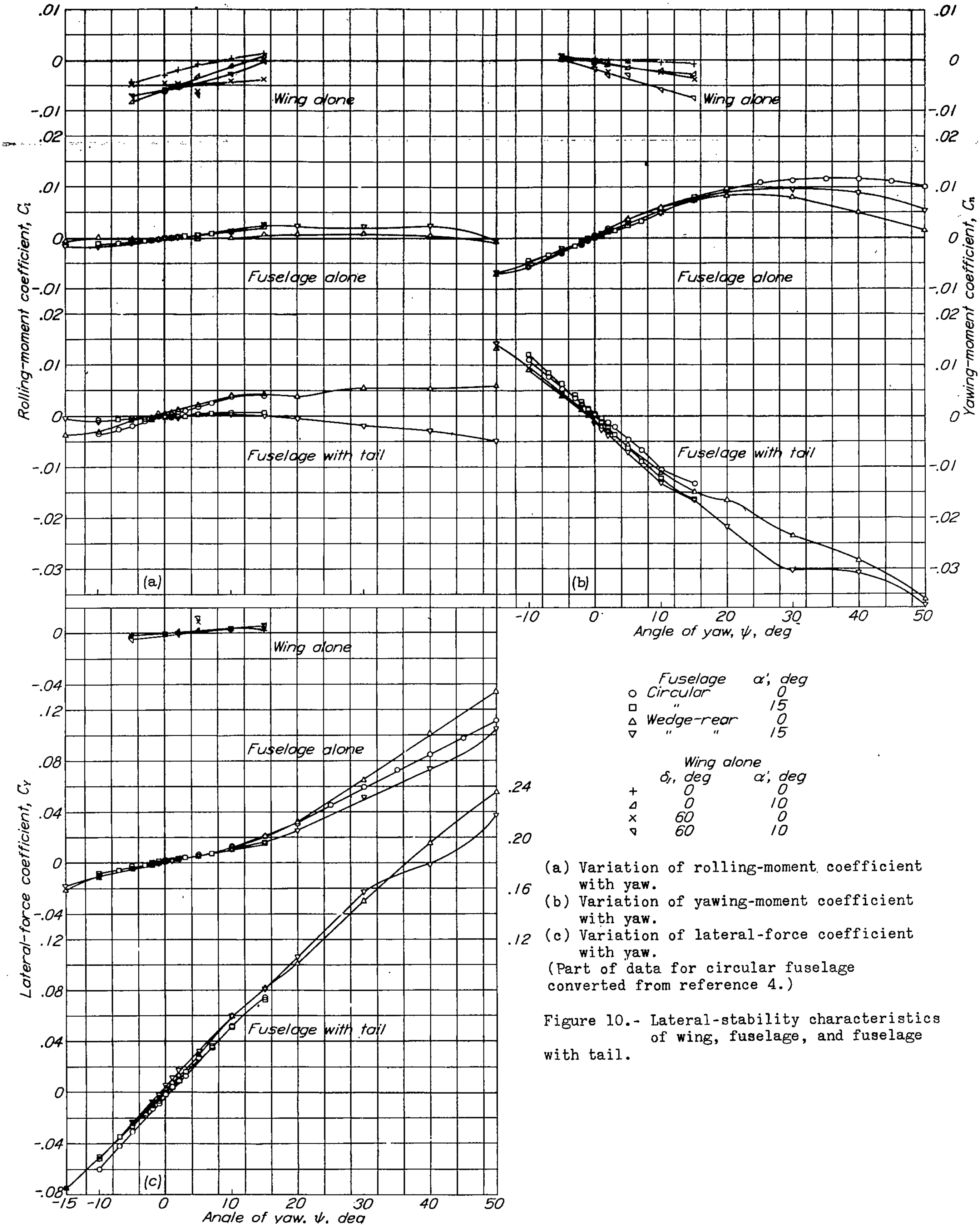

(a) Variation of rolling-moment coefficient with yaw.
(b) Variation of yawing-moment coefficient with yaw.
(c) Variation of lateral-force coefficient with yaw.
(Part of data for circular fuselage converted from reference 4.)

Figure 10.- Lateral-stability characteristics of wing, fuselage, and fuselage with tail.

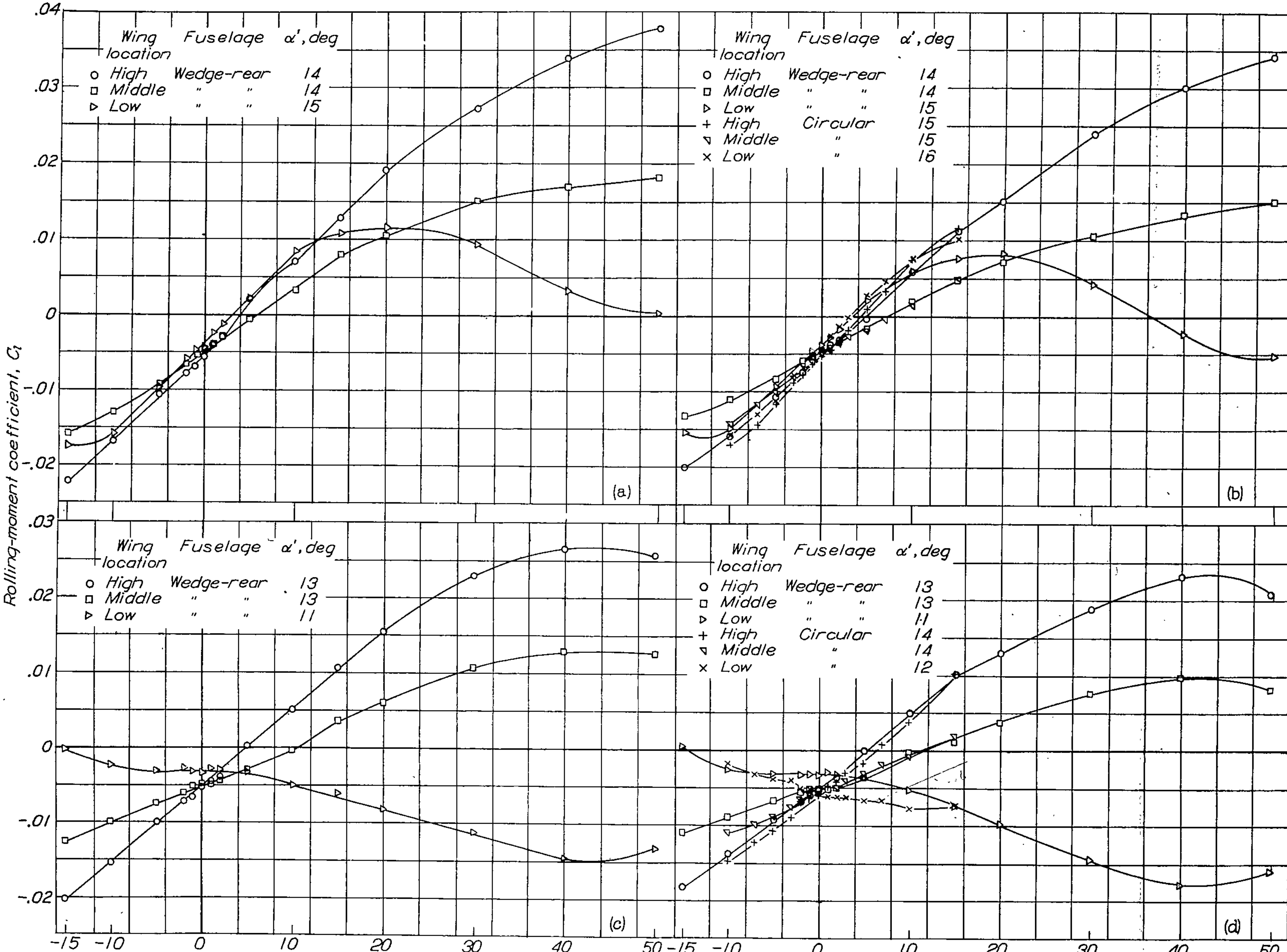

(a) Tail off, $\delta_f = 0^\circ$ (b) Tail on, $\delta_f = 0^\circ$ (c) Tail off, $\delta_f = 60^\circ$ (d) Tail on, $\delta_f = 60^\circ$

Figure 11.- Variation of rolling-moment coefficient with yaw. NACA 23012 wing with fuselage, $\Lambda = 4.75^\circ$. (Data for circular fuselage converted from reference 2.)

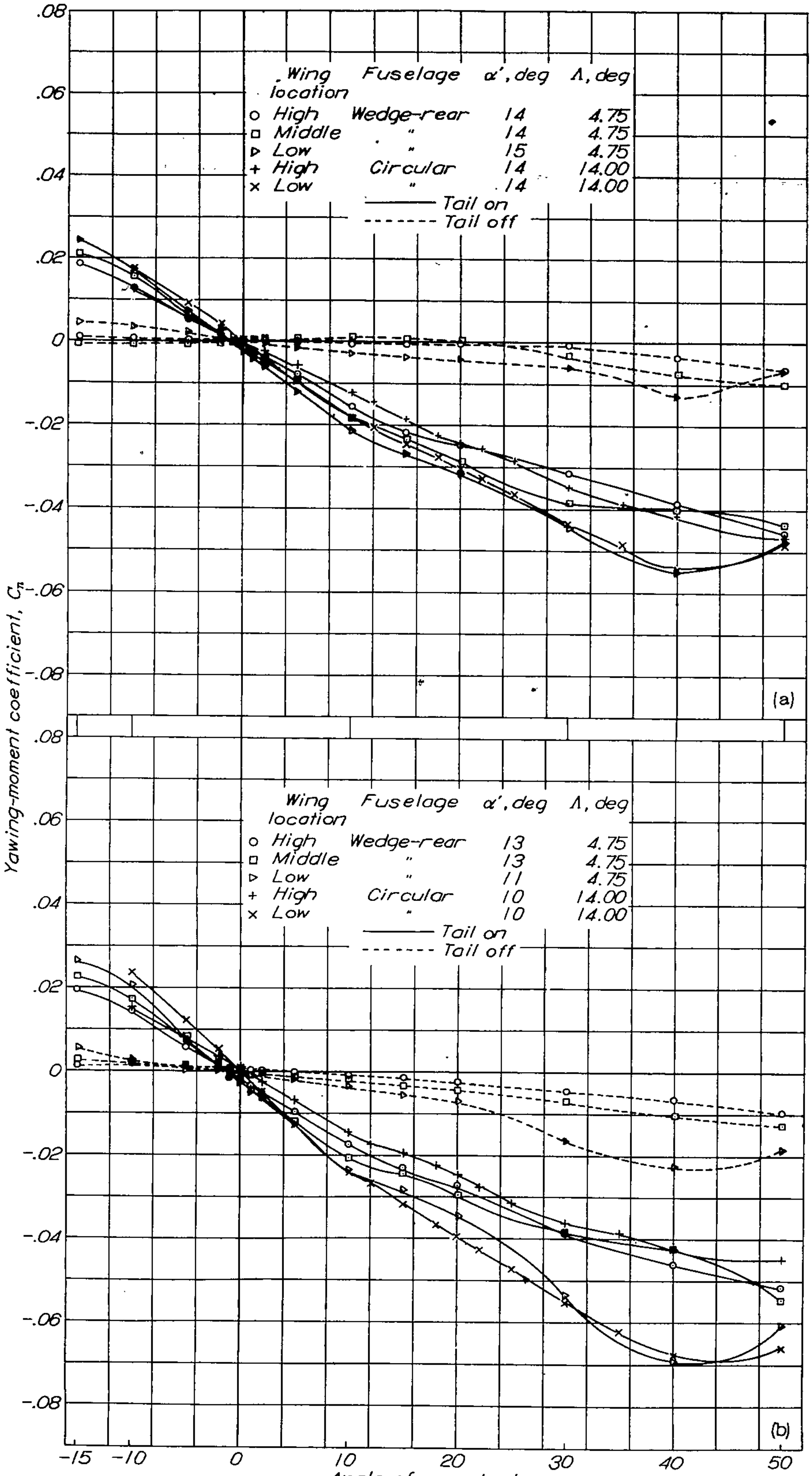

Figure 12.- Variation of yawing-moment coefficient with yaw. NACA 23012 wing with fuselage. (Data for circular fuselage converted from reference 5.)

(a) $\delta_f = 0°$

(b) $\delta_f = 60°$

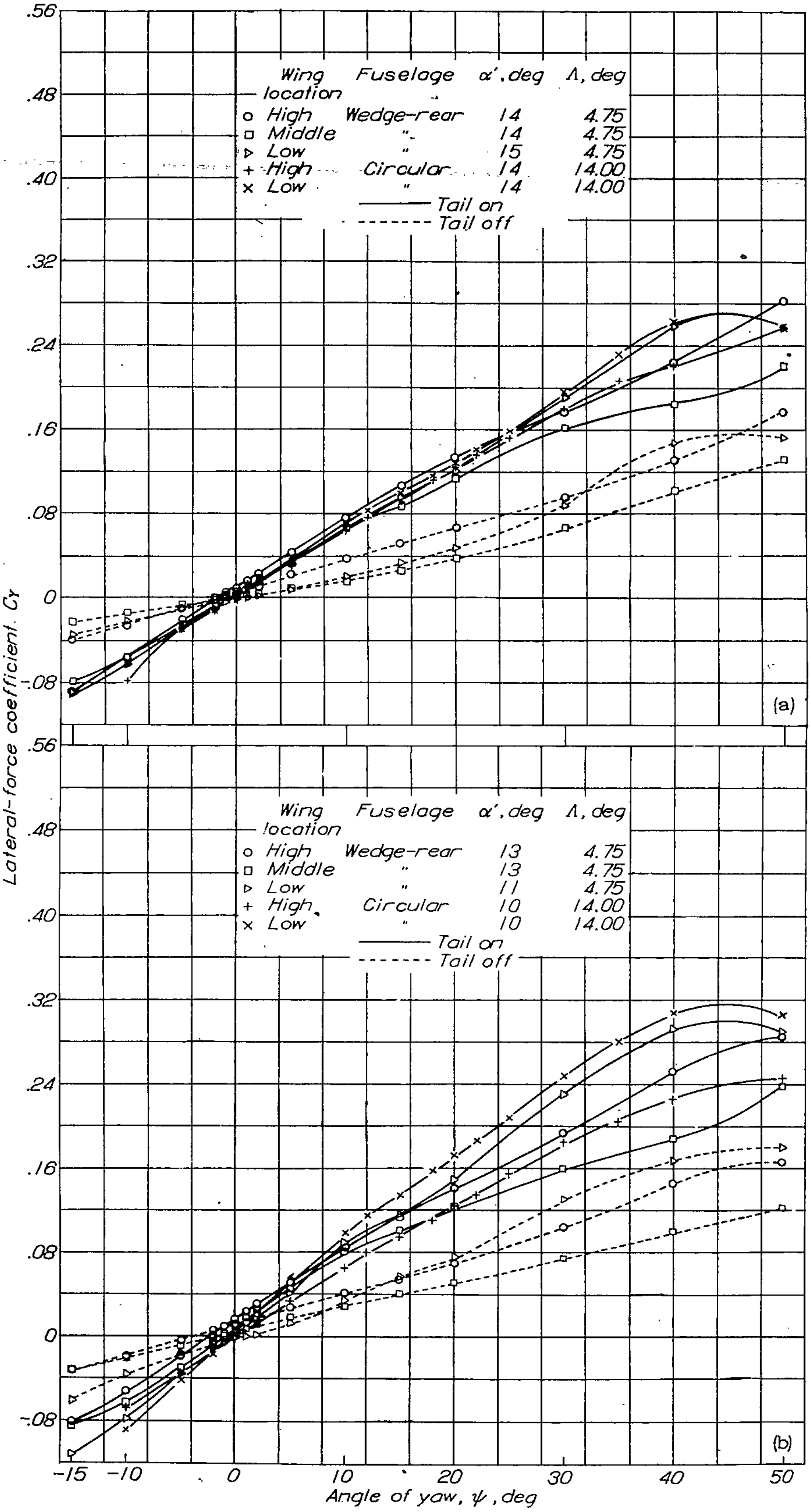

Figure 13.- Variation of lateral-force coefficient with yaw. NACA 23012 wing with fuselage. (Data for circular fuselage converted from reference 5.)

(a) $\delta_f = 0°$

(b) $\delta_f = 60°$